Verification of Size Invariance in DNN Activations Using Concept Embeddings

Gesina Schwalbe

Verification of Size Invariance in DNN Activations using Concept Embeddings*

Gesina Schwalbe[1,2][0000−0003−2690−2478]

[1] Continental AG, Regensburg, Germany
gesina.schwalbe@continental-corporation.com
[2] Cognitive Systems, University of Bamberg, Bamberg, Germany

Abstract. The benefits of deep neural networks (DNNs) have become of interest for safety critical applications like medical ones or automated driving. Here, however, quantitative insights into the DNN inner representations are mandatory [10]. One approach to this is *concept analysis*, which aims to establish a mapping between the internal representation of a DNN and intuitive semantic concepts. Such can be sub-objects like human body parts that are valuable for validation of pedestrian detection. To our knowledge, concept analysis has not yet been applied to large object detectors, specifically not for sub-parts. Therefore, this work first suggests a substantially improved version of the Net2Vec approach [5] for post-hoc segmentation of sub-objects. Its practical applicability is then demonstrated on a new concept dataset by two exemplary assessments of three standard networks, including the larger Mask R-CNN model [9]: (1) the consistency of body part similarity, and (2) the invariance of internal representations of body parts with respect to the size in pixels of the depicted person. The findings show that the representation of body parts is mostly size invariant, which may suggest an early intelligent fusion of information in different size categories.

Keywords: Concept embedding analysis · MS COCO · Explainable AI.

1 Introduction

The high performance and flexibility of deep neural networks (DNNs) makes them interesting for many complex computer vision applications. This includes ethically involved or safety critical fields where silent biases can become a matter of unfairness, or even life-threatening decisions. Hence, responsible artificial intelligence is required, allowing for thorough assessments of trained DNNs [1]. For example in the area of automated driving, quantitative insights into the inner representation of trained DNNs are mandatory [10].

One step towards this direction is the research area of *concept (embedding) analysis* [5,11], that started with the work in [2] in 2017. Supervised concept analysis aims to answer the question how (well) information on a visual semantic

* The research leading to these results was partly funded by the German Federal Ministry for Economic Affairs and Energy within the project "KI-Absicherung".

concept is embedded in the intermediate output of one layer of a trained DNN. A concept can be, e.g., a texture, material, scene, object, or object part [2], and should be given as samples with binary annotations. The question is answered by training a simple model to predict the concept from the layer output, with simplicity ensuring interpretability [2,11]. Once these *concept models* are obtained, several means for verification open up: The embedding quality can be measured as the prediction quality of the concept model; if a similarity measure for concept models is available, semantic relations between concepts can be validated (e.g. legs are similar to arms) [5]; and lastly, if the information embedding can be represented as a vector in the latent space, one can use sensitivity analysis to investigate dependencies of outputs on certain concepts [11]. The vector can be the normal vector of a linear model, or the center of a cluster, and is called the embedding of the concept [5].

While concept analysis opens up a wide variety of verification options, existing methods suffer from some limitations. For one, the methods are either restricted to image-level concepts, or, like Net2Vec [5], report poor results for part objects. But part objects, such as human body parts, are substantial to verify logical plausibility of pedestrian detectors needed for automated driving. This brings up the second issue: To our knowledge, existing proposals have not been evaluated on large networks like standard object detectors. Concretely, we uncovered some severe performance limitations of Net2Vec that impede application to state-of-the-art sized DNNs or larger concept datasets than the original Broden dataset proposed in [2].

In order to overcome the practical issues, this paper suggests some substantial improvements to the Net2Vec method, demonstrated on a new large MS COCO [15] based concept dataset for human body parts. The applicability of concept analysis for simple verification is demonstrated by exemplary assessment of three networks with different sizes, tasks, and training data (AlexNet, VGG16, and Mask R-CNN [9]). Concretely, the semantic similarity of different concepts is validated, and it is checked whether the internal representation of the networks is biased towards one size category (i.e. distance to the camera). Interestingly, our findings suggest that convolutional DNNs are not biased towards one size. Instead, from early layers onwards, they use an efficient common representation for instances of the same part object but different sizes. The main contributions of this paper are:

- A Net2Vec-based concept analysis approach that can deal with large models and large concept datasets is presented and demonstrated. It is found to considerably surpass the state-of-the-art for object part concepts.
- The first evaluation of size invariance of the internal representations of convolutional DNNs is conducted.
- For this, an approach is presented to estimate the pixel size of persons in 2D images from skeletal annotations, which can be used for concept mask generation.

After a revision of concept analysis methods in Sec. 2, our approach is introduced in Sec. 3. Finally, in Sec. 4 it is validated and used for the exemplary assessment.

2 Related Work

An early approach to supervised concept analysis was NetDissect by Bau et al. [2]. They associated single convolutional filters with semantic concepts, and provided the Broden dataset, a combined dataset featuring a wide variety of concepts. Building upon NetDissect, Net2Vec [5] expanded from single filters to combinations of filters and trains a 1×1 convolution to predict concept masks from latent space outputs. Intuitively, the weight vector of the convolution, the concept embedding vector, encodes the direction within the layer output space that adds the concept. The authors investigate the similarity of different concepts via cosine similarity of their concept vectors. Similarly, TCAV by Kim et al. [11] trains linear models but using a support vector machine on the complete latent space output for binary classification instead of segmentation. The authors suggest to use partial directional derivatives along the concept vectors to assess how outputs depend on concepts in intermediate layers. Future work may investigate how this can be applied to concept segmentation instead of concept classification. Other than the previous linear model approaches, SeVec [8] uses a k-means clustering approach, demonstrated on a dataset other than Broden, but again only on image-level concepts and with a manual step in the process. The Net2Vec-based proof of concept in [19] uses a small concept dataset for traffic sign letters. This work also details the value of concept analysis for safety assessment, and suggests that a mismatch of concept size and receptive field of concept models can cause a texture bias, that is, predictions purely based on texture. This is investigated for larger nets in this paper.

More relevant for inspection than requirements verification purposes, unsupervised concept analysis approaches aim to find and visualize repetitive concepts in the intermediate output of a DNN. A simple example is feature visualization [16], where noise is optimized to maximally activate a convolutional filter. ACE [7] instead uses super-pixels as concept candidates, which are then clustered by their latent space proximity. In the direction of representation disentanglement, [21] introduced a measure for the completeness of a set of concept vectors with respect a given task. Their idea is that post-hoc adding a semantic bottleneck with unit vectors aligned to the concepts should not decrease the model performance. Similarly, but with invertible DNNs instead of linear maps, the recent work in [4] tries to find a bijection of a latent space to a product of semantically aligned sub-spaces (and a residual space).

Experiments so far have been conducted on small resolution image datasets like the 224×224 pixels of the Broden [2,5,11]and ImageNet [8] data or less [19], and have not yet been applied to large models or object detectors.

3 Approach

This section introduces our concept analysis approach with its modifications to the Net2Vec concept analysis method, and an approach to estimate the body size in pixels for persons in 2D images from skeletal annotations. Size estimation is

later used to generate ground truth segmentation masks for body part concepts, and to categorize them by size.

3.1 Concept Embedding Analysis

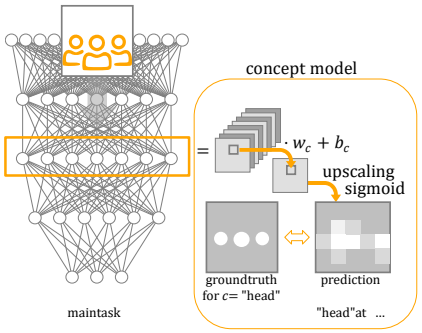

Fig. 1. Illustration of the used concept analysis approach. For a concept c, here "head", it predicts binary segmentation masks from convolutional activation maps via (1) a 1-filter convolution with kernel w_c and bias b_c, (2) bilinear upscaling (here depicted using nearest pixel upscaling), and finally (3) normalization.

Our method is illustrated in Figure 1. As a foundation, the Net2Vec [5] approach was chosen. It allows to localize non-image-level concepts like object parts in convolutional activation maps by predicting binary segmentation masks. For this the spatial resolution of the convolutional layers is used: The mask predictor is a 1×1 convolution followed by bilinear upscaling, then sigmoid normalization (and, for binarizing, thresholding at 0.5). For comparability, the quality measure set intersection over union (set IoU) is adopted which divides the total area of intersections by the total area of unions between the binary ground truth masks M_i and the predicted segmentation masks M_i^{pr} (binarized at 0.5):

$$\text{set IoU}\left((M_i)_i, (M_i^{\text{pr}})_i\right) = \frac{\sum_i \sum M_i \cap (M_i^{\text{pr}} > 0.5)}{\sum_i \sum M_i \cup (M_i^{\text{pr}} > 0.5)} \,. \tag{1}$$

We here took the mean of batch-wise set IoU values. It must be noted that the set IoU measure penalizes errors on small objects more than on large ones, and it suffers under low resolution of activation maps. Below, four further limitations of Net2Vec are collected and our countermeasures explained.

Most notably, Net2Vec uses denoising of activation maps with a ReLU suggested in [2]. The threshold is calculated to keep the 0.5% highest activations. This requires to load activations of the complete dataset into memory at once, which is infeasible both for large models and large datasets. Experiments showed that denoising makes no noticeable difference, hence it is skipped.

Next, to push the decision boundary of the model towards a value of 0.5, Net2Vec uses a binary cross-entropy (BCE) loss with per-class-weights where each weight is the mean proportion of pixels of the opposite class. Obtaining the weight is an expensive pre-processing step. Here we found that global weighting could be replaced either by calculating weights batch-wise, or using an unweighted Tversky loss [18]—also called Dice or F1 loss—that directly optimizes

the F1 score of the segmentation per $h \times w$ image ("$\cdot$" pixel-wise):

$$\text{Dice loss}\,(M, M^{\text{pr}}) = 1 - \frac{2\sum M \cdot M^{\text{pr}}}{\sum M + \sum M^{\text{pr}}} \quad \text{for } M, M^{\text{pr}} \in [0,1]^{h \times w}. \tag{2}$$

Further, the original method reports average set IoU values lower than 0.05 for part objects, which we could confirm. This can be achieved by constantly predicting white masks (1 for all pixels). In a series of experiments we found settings fixing this: We use a Tversky loss, Adam optimizer [12] instead of stochastic gradient descent (SGD), with a batch size of 8 instead of 64, and learning rate of 10^{-3} rather than 10^{-4}.

Another modification used in some experiments is *adaptive kernel size*. The original Net2Vec method uses a 1×1 kernel, so each prediction only has a spatial context of one pixel. As found in [19], this may be too small for larger concepts and layers with higher resolution, and possibly leads to a texture bias [6]. Following [19], this can be mitigated using a kernel size that covers an area of the expected size of the concept, assuming low size variance. Note that this may improve performance of a concept model, but destroys comparability amongst models of differently sized concepts due to incompatible kernel shapes.

3.2 Distance Category Estimation

Formulas for total height
$1 \cdot$ `bbox_width/_height`
$1.1 \cdot$ `body_height`
$2.4 \cdot$ `hip_to_shoulder`
$7 \cdot$ `head_height`
$1.485 \cdot$ `leg` $\cdot \frac{h}{h-0.433}$
$2.77 \cdot$ `upper_leg` $\cdot \frac{h}{h-0.405}$
$3.075 \cdot$ `lower_leg` $\cdot \frac{h}{h-0.501}$
$3.72 \cdot$ `upper_arm` $\cdot \frac{h}{h-0.449}$
$4.46 \cdot$ `lower_arm` $\cdot \frac{h}{h-0.569}$

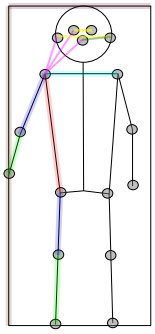

Formulas for derived lengths	
`body_height`	$\approx$ `leg`* + `hip_to_shoulder`* + `shoulder_to_eye`*/`_ear`*/`_nose`
	$\approx$ `arm` + `shoulder_width`
`leg`	$\approx$ `lower_leg` + `upper_leg`
`arm`	$\approx$ `lower_arm` + `upper_arm`
`head_height`	$\approx 1.1 \cdot$ `head_width`
	$\approx \frac{8}{7}$ `head_depth`
`head_width`	$\approx$ `ear_to_opposite_ear`
	$\approx 2.5 \cdot$ `eye_to_eye`
`head_depth`	$\approx 2 \cdot$ `ear_to_eye`*
	$\approx \frac{7}{4}$ `ear_to_nose`

* involved keypoints must be on the same side

Fig. 2. Used keypoints and links with formulas to estimate the total body height of a person from link lengths and assumed "standard" height h in meters.

Assume an image dataset is given that provides 2D skeletal information of persons (cf. Figure 2), possibly bounding boxes, but no depth information. The goal of this approach is to estimate and categorize the body size of a person depicted in a 2D image in pixels, given only lengths between keypoints. The challenges are that keypoint information may be incomplete due to occlusion or cropping, and that 2D projected lengths may be inaccurately short. Thus, redundant calculation of body size from as many link types as possible is needed. One

major drawback of this method is that assumptions on "standard" proportions must be made. This cannot be overcome without additional information. Despite that, it was found that the approach yields surprisingly good and intuitive results, with errors not infringing the quality of body size categorization.

The following sources were used to relate the true length l of (combinations of) keypoint links to the true body height h: arts for facial and head-to-body proportions [14]; standard educational material relating the wrist-to-wrist span [3]; and linear models used in archeology to estimate the body size from single long bones [14]. For long bone relations, the mean model parameters were taken between genders. Relations involving approximate `body_height` and bounding box (`bbox`) dimensions were estimated manually. The resulting relation models are all of the linear nature $h = s \cdot l + c$ for some slope s, and offset c in meters. Given the downscaled length $l' = f \cdot l$ in pixels, the formula for the downscaled body size is $f \cdot h = l' \cdot \frac{h}{h-c}$. If c is non-zero, a "standard" real person size h must be assumed, which was set to 1.7 m following [14]. The final formulas are shown in Figure 2. Whenever one value has several estimation results, the maximum was used to cope with possible length shortenings due to 2D projection.

The formulas were now leveraged to sort annotations into four size categories. These were chosen such that in each the minimum and maximum estimated size do not differ by more than a factor of two. Very small and very large persons were discarded. The resulting size categories with their range of relative sizes are: *far* in $[0.2, 0.38]$, *middle* in $[0.38, 0.71]$, *close* in $[0.71, 1.33]$, and *very close* in $[1.33, 2.5]$. Categories are depicted in Figure 3.

4 Experiments

After detailing our experiment settings, this section will validate the used approach including hyperparameters (Sec. 4.1), then conduct exemplary assessments of embedding quality and semantics (Sec. 4.2), as well as size bias (Sec. 4.3).

For the experiments, we chose three networks of different size, training objective, and training dataset, with pretrained weights from the torchvision model zoo[3]: ImageNet-trained classifiers VGG16 [20] and AlexNet [13], and the object detector Mask R-CNN [9] trained on MS COCO. As layers we chose the activated convolutional output before each downsampling step except the first. In case of Mask R-CNN we considered the output of each residual grouping in the backbone and the feature pyramid. For concepts we selected a set of five large and small concepts that are common to the Broden and MS COCO datasets: leg, arm, foot and hand (for COCO approximated via ankle and wrist keypoints), and eye. Images were zero-padded to square size then resized to 400×400 respectively 224×224 (VGG16, AlexNet) pixels to avoid feature distortion. Ground truth masks on concepts for MS COCO images were generated by drawing links (leg, arm) respectively points (foot, hand, eye) of width 0.025 times the image height or times the body size if this can be estimated (see Figure 5). Intermediate outputs of the DNNs were cached with bi-float 16 precision to speed up

[3] https://pytorch.org/vision/stable/models.html

experiments, except for the very large Mask R-CNN feature pyramid blocks 0 and 1, and backbone layer 1. On cached layers, concept model training was done with 5-fold cross-validation. The original train-test splits were used.

4.1 Validation of the Proposed Methods

Size Distribution in MS COCO To validate the size estimation approach, an analysis of the size distribution on the popular MS COCO dataset was conducted. The size of an annotation cannot be estimated if it provides no keypoints (very small persons and crowds) or only disconnected keypoints. Nevertheless, size estimations could be made for a decent proportion of the annotations in both training and test set (ca. 46%), see Figure 3. Also, for each chosen body part, a sufficient amount of annotations is available in size categories *far*, *middle*, and *close*: more than 10,000 in the train, and 300 in the test set. These categories were thus used for experiments. Training and test set were found to be similarly distributed, with significantly more keypoint annotations estimated far than close. This suggests, that the total amount of positive pixels for masks of small far body parts is similar to that of large close ones.

Improvement of Net2Vec Settings for the concept analysis approach were needed that (1) work for large models and datasets (no expensive thresholds and weights), and (2) work for part objects. First, the necessity to threshold the activation maps was disproved: Skipping it had no effect on the test performance. Then, without thresholding, a series of experiments was conducted comparing different optimizers (SGD, Adam), batch sizes (bs), learning rates (lr), and losses (globally weighted BCE, batch-wise weighted BCE, and Tversky). Each setting was evaluated on AlexNet and VGG16, on all selected layers and concepts, using the original Broden dataset [2]. Firstly, the better optimizer was chosen, then the better batch-size and learning rate combination, and lastly losses were compared. The consistently best and stable setting proved to be Adam optimizer with lr 10^{-3}, bs 8, with maximum five epochs due to fast convergence. Find a comparison to the baseline for AlexNet in Figure 3 (VGG16 similar).

4.2 Embedding Quality and Similarity Validation

Two applications of concept analysis are to verify sufficient embedding qualities, and to use the similarity measure on the concept models for validation of semantic relations. For this, concept models for all chosen concepts, networks, and layers were trained on the complete MS COCO concept dataset. Performance results are depicted in Figure 6 (size category *all*). As before, the variance was very low, evidencing good convergence of the linear concept models. Convincing embedding qualities were found except for the small concepts hand and foot in small networks. This may origin from the approximate and noisy ground truth, and the higher set IoU penalties for low resolution. In general, later layers with low resolution showed the best embedding results, indicating that body parts are relatively complex concepts. These may require larger network structures,

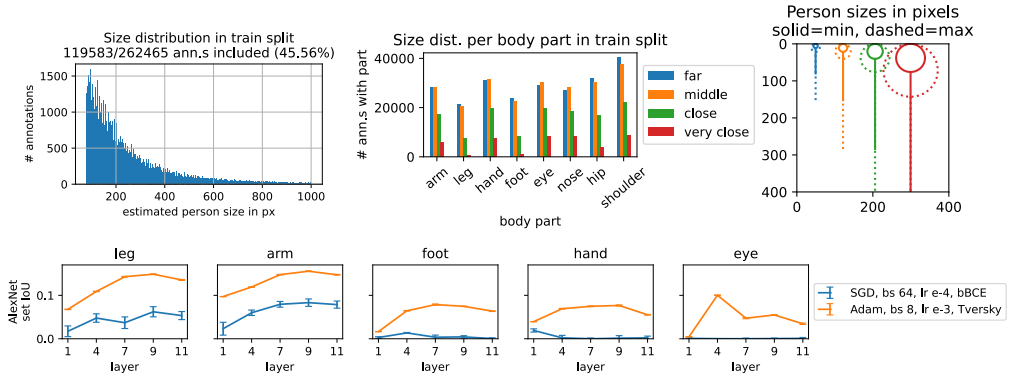

Fig. 3. *Top:* Distribution by estimated person size of all annotations (*left*) and per body part (*center*) for COCO train images (padded to square size and resized to 400 × 400 px); used person size categories are illustrated on the *right*. *Bottom:* Performance comparison of used settings with Net2Vec baseline (cf. [5, Fig. 2]). Best viewed in color.

since Mask R-CNN significantly surpassed AlexNet and VGG16. Some exemplary output for Mask R-CNN is shown in Figure 6.

Next, the concept model similarities were measured as the mean cosine similarity between the normal vectors of the models, shown in Figure 4. Cosine similarity $\frac{a \cdot b}{\|a\| \cdot \|b\|}$ of vectors $a, b \in \mathbb{R}^n$ is the cosine of the angle between the vectors, with 1 meaning 0° angle, and -1 meaning 180°. The results show intuitive relations between the concepts: No similarity values were below zero, so no body part concepts are mutually exclusive. And eye is most different from the other parts, while hand and arm are more closely related, similarly leg and foot. Interestingly, in the later low-resolution layers concepts were more dissimilar, so better distinguishable, explaining the better performance here.

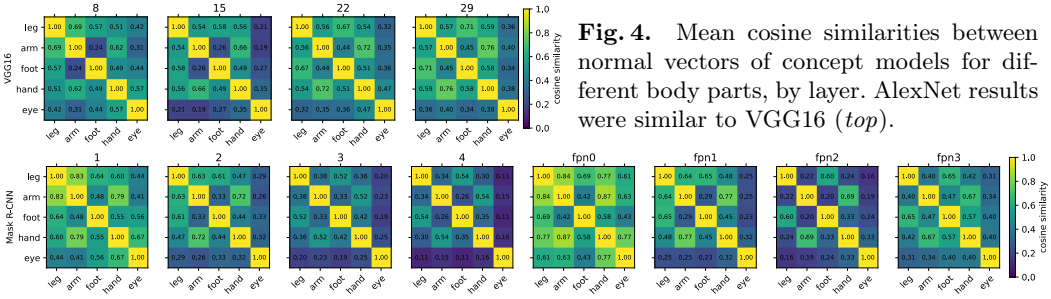

Fig. 4. Mean cosine similarities between normal vectors of concept models for different body parts, by layer. AlexNet results were similar to VGG16 (*top*).

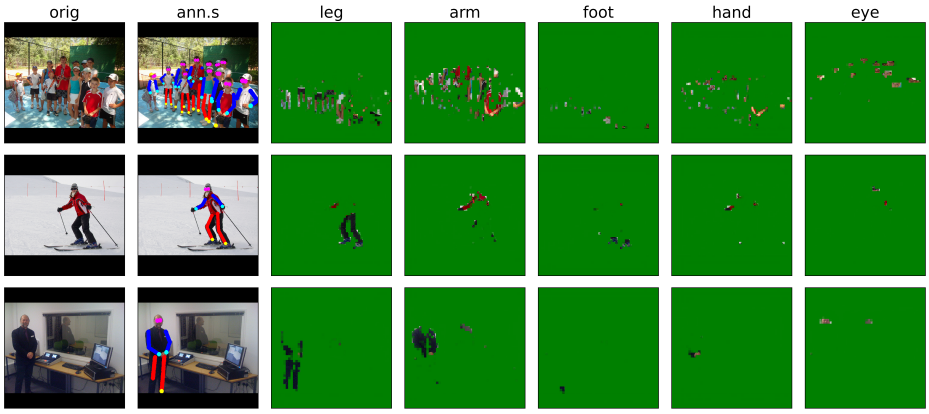

Fig. 5. Overlay (green) of segmentation masks predicted by the mean concept model of Mask R-CNN backbone layer block 3. Original images are shown in first column, generated ground truth annotations in second column in different colors. Mean is taken over normalized concept vectors, cf. [17]. Masks are upsampled using nearest rule to demonstrate resolution. Note how predicted masks clearly correlate with the ground truth instead of being purely white. Images are taken from test set (MS COCO `val2017`). For the used images thanks to: top: Oleg Klementiev http://farm5.staticflickr.com/4115/4906536419_6113bd7de4_z.jpg © CC BY 2.0; middle: Nick Webb http://farm8.staticflickr.com/7015/6795644157_f019453ae7_z.jpg © CC BY 2.0; bottom: Yandle http://farm4.staticflickr.com/3179/2986591710_d76622fdf0_z.jpg © CC BY 2.0

4.3 Correlations of Person Size and Segmentation Quality

The last series of experiments means to investigate the following questions: 1) Does the internal representation of a concept differ for different sizes of the concept? And is there a safety critical bias towards one size (i.e. distance from the camera)? 2) Is adaptive kernel size needed to avoid texture bias? A yes to 1) would suggest that different and better embeddings can be found if concept information is assessed separately for each size category. Then, especially for larger size categories, adaptive kernel sizes might be necessary. To answer the questions, results on a test set restricted to one size category were collected on the MS COCO concept data. This was done and compared for concept models trained on the complete dataset (all nets), and models trained on the respective size category either with 1×1 or adaptive kernel size (AlexNet, VGG16). Adaptive kernel sizes were chosen to cover the following areas relative to the mean person size of the size category (in height×width): 0.3×0.1 for leg, 0.2×0.15 for arm, 0.1×0.1 for foot and hand, and 0.04×0.04 for eye. The two main results were: The internal representation of body parts seems to be mostly size invariant, and adaptive kernel sizes are not necessary.

Results In Figure 6 the performance of concept models trained on *all* data was compared for different test subsets. The differences between size categories did not exceed what was expected from the different set IoU penalties, so no bias

could be found here. Since a concept model trained on all data may not be the optimal one for a size, we also compared the *all* models to models solely trained on the respective size category, see Figure 7. This showed that a restricted training set may even decrease test results, indicating that at least parts of the internal representation used for the different sizes must be shared. To substantiate that, the normal vectors of the linear models for the different size categories were compared. In the best performing layers the restricted size categories had high cosine similarity (over 0.7) to *all*, with *far* deviating the most. However, *all* could not be represented as a linear combination of the sub-sizes, and cosine similarities of least squares solutions did not top 0.95. So, some information even seems to get lost when training only on single size categories. Lastly, results on single size categories were also compared to adaptive kernel size results in Figure 7. Adaptive kernel size would show some improvements but the best layer rarely changed.

5 Conclusion

This paper proposed an efficient concept analysis approach that is fit for practical application to large networks and datasets, and to object part concepts. It was demonstrated how this method can be used to assess consistency and size bias in the internal representations of a DNN. For this, a size estimation method from 2D skeletal data is proposed together with a new concept dataset based on MS COCO keypoint annotations. Our assessment results suggest that the representations within standard models AlexNet, VGG16, and Mask R-CNN are mostly invariant to different sizes respectively camera distances. Despite drawbacks of the used set IoU metric, concept analysis is shown to be a promising approach for verification and validation of deep neural networks. Future work will investigate further assessment possibilities arising from post-hoc explainable access to DNN intermediate output. This can, e.g. , be used to test or formally verify logical properties that are formulated on the enriched DNN output.

References

1. Arrieta, A.B., Rodríguez, N.D., Ser, J.D., Bennetot, A., Tabik, S., Barbado, A., García, S., Gil-Lopez, S., Molina, D., Benjamins, R., Chatila, R., Herrera, F.: Explainable artificial intelligence (XAI): Concepts, taxonomies, opportunities and challenges toward responsible AI. Information Fusion **58**, 82–115 (2020)
2. Bau, D., Zhou, B., Khosla, A., Oliva, A., Torralba, A.: Network dissection: Quantifying interpretability of deep visual representations. In: Proc. 2017 IEEE Conf. Comput. Vision and Pattern Recognition. pp. 3319–3327. IEEE Computer Society (2017). https://doi.org/10.1109/CVPR.2017.354
3. De Brabandere, S.: Human body ratios. Scientific American (Bring Science Home) (Mar 2017), https://www.scientificamerican.com/article/human-body-ratios/
4. Esser, P., Rombach, R., Ommer, B.: A disentangling invertible interpretation network for explaining latent representations. In: Proc. 2020 IEEE Conf. Comput. Vision and Pattern Recognition. pp. 9220–9229 (Jun 2020)

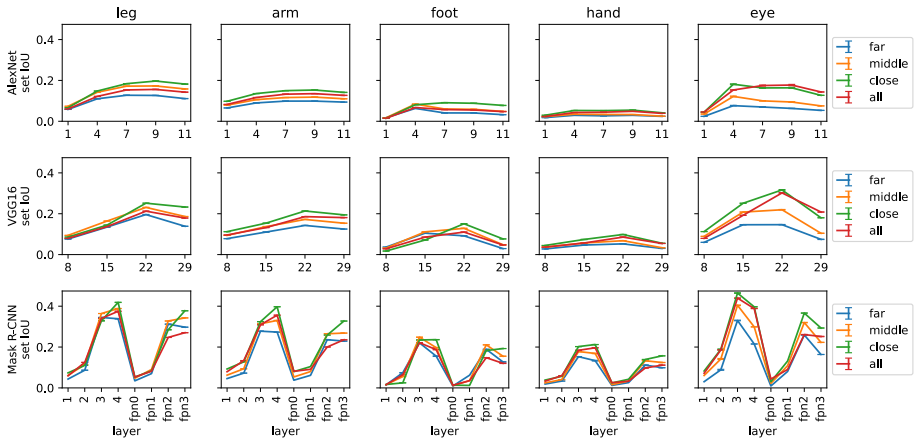

Fig. 6. Test set IoU results of concept models trained on the complete dataset, by layer, annotation size category, model (top to bottom), and concept (left to right). Note that standard deviations are marked but negligible. Best viewed in color.

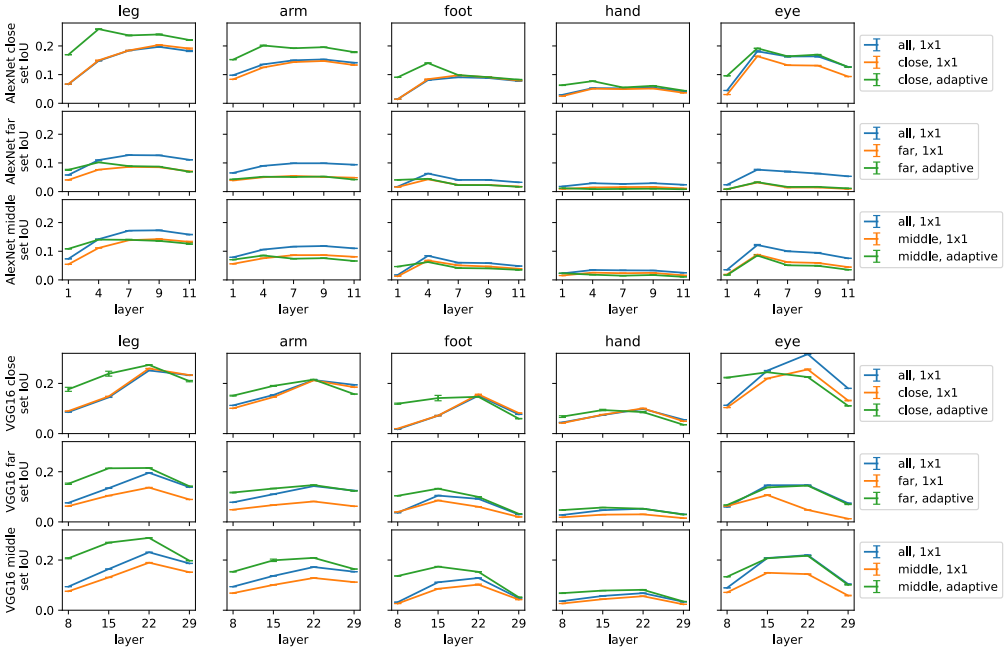

Fig. 7. Test set IoU results of concept models trained on a size subset by layer and kernel setting. Results were obtained on the test set restricted to the respective training size category. Results for the models trained on all data are added for comparison, cf. Figure 6. Best viewed in color.

5. Fong, R., Vedaldi, A.: Net2Vec: Quantifying and explaining how concepts are encoded by filters in deep neural networks. In: Proc. 2018 IEEE Conf. Comput. Vision and Pattern Recognition. pp. 8730–8738. IEEE Computer Society (2018)
6. Geirhos, R., Rubisch, P., Michaelis, C., Bethge, M., Wichmann, F.A., Brendel, W.: ImageNet-trained CNNs are biased towards texture; increasing shape bias improves accuracy and robustness. In: Proc. 7th Int. Conf. Learning Representations. OpenReview.net (2019)
7. Ghorbani, A., Wexler, J., Zou, J.Y., Kim, B.: Towards automatic concept-based explanations. In: Advances in Neural Information Processing Systems 32. pp. 9273–9282 (2019)
8. Gu, J., Tresp, V.: Semantics for global and local interpretation of deep neural networks. CoRR **abs/1910.09085** (Oct 2019), http://arxiv.org/abs/1910.09085
9. He, K., Gkioxari, G., Dollár, P., Girshick, R.: Mask R-CNN. In: 2017 IEEE International Conference on Computer Vision (ICCV). pp. 2980–2988 (Oct 2017)
10. ISO/TC 22/SC 32: ISO 26262-6:2018(En): Road Vehicles — Functional Safety — Part 6: Product Development at the Software Level, ISO 26262:2018(En), vol. 6. International Organization for Standardization, second edn. (Dec 2018)
11. Kim, B., Wattenberg, M., Gilmer, J., Cai, C., Wexler, J., Viegas, F., Sayres, R.: Interpretability beyond feature attribution: Quantitative testing with concept activation vectors (TCAV). In: Proc. 35th Int. Conf. Machine Learning. Proceedings of Machine Learning Research, vol. 80, pp. 2668–2677. PMLR (Jul 2018)
12. Kingma, D.P., Ba, J.: Adam: A method for stochastic optimization. In: Proc. 3rd Int. Conf. Learning Representations (2015)
13. Krizhevsky, A.: One weird trick for parallelizing convolutional neural networks. CoRR **abs/1404.5997** (2014), http://arxiv.org/abs/1404.5997
14. Larson, D.: Standard proportions of the human body (Jan 2014), https://www.makingcomics.com/2014/01/19/standard-proportions-human-body/
15. Lin, T.Y., Maire, M., Belongie, S.J., Hays, J., Perona, P., Ramanan, D., Dollár, P., Zitnick, C.L.: Microsoft COCO: Common objects in context. In: Proc. 13th European Conf. Computer Vision - Part V. Lecture Notes in Computer Science, vol. 8693, pp. 740–755. Springer International Publishing (2014)
16. Olah, C., Mordvintsev, A., Schubert, L.: Feature visualization. Distill **2**(11) (Nov 2017). https://doi.org/10.23915/distill.00007
17. Rabold, J., Schwalbe, G., Schmid, U.: Expressive explanations of DNNs by combining concept analysis with ILP. In: KI 2020: Advances in Artificial Intelligence. pp. 148–162. Lecture Notes in Computer Science, Springer International Publishing (2020). https://doi.org/10.1007/978-3-030-58285-2_11
18. Salehi, S.S.M., Erdogmus, D., Gholipour, A.: Tversky loss function for image segmentation using 3D fully convolutional deep networks. In: Proc. 8th Int. Workshop Machine Learning in Medical Imaging. vol. 10541, pp. 379–387. Springer (2017)
19. Schwalbe, G., Schels, M.: Concept enforcement and modularization as methods for the ISO 26262 safety argumentation of neural networks. In: Proc. 10th European Congress Embedded Real Time Software and Systems (Jan 2020), https://hal.archives-ouvertes.fr/hal-02442796
20. Simonyan, K., Zisserman, A.: Very deep convolutional networks for large-scale image recognition. In: Proc. 3rd Int. Conf. Learning Representations (2015)
21. Yeh, C.K., Kim, B., Arik, S., Li, C.L., Pfister, T., Ravikumar, P.: On completeness-aware concept-based explanations in deep neural networks. In: Advances in Neural Information Processing Systems 33. vol. 33, pp. 20554–20565 (2020)